Naval Research Laboratory

Stennis Space Center, MS 39529-5004

Application of a Shelf-Scale Model to Wave-Induced Circulation: Alongshore Currents on Plane and Barred Beaches

CHERYL ANN BLAIN

Ocean Dynamics and Prediction Branch
Oceanography Division

MARK COBB

Sverdrup Technologies, Inc.
Stennis Space Center, MS

March 11, 2003

REPORT DOCUMENTATION PAGE

Form Approved
OMB No. 0704-0188

1. REPORT DATE *(DD-MM-YYYY)*	2. REPORT TYPE	3. DATES COVERED *(From - To)*
March 11, 2003	Formal	October 29-31, 2002

4. TITLE AND SUBTITLE

Application of a Shelf-Scale Model to Wave-Induced Circulation: Alongshore Currents on Plane and Barred Beaches

5a. CONTRACT NUMBER

5b. GRANT NUMBER

5c. PROGRAM ELEMENT NUMBER
602435N

6. AUTHOR(S)

Cheryl Ann Blain and Mark Cobb*

5d. PROJECT NUMBER

5e. TASK NUMBER
BE-435-028

5f. WORK UNIT NUMBER

7. PERFORMING ORGANIZATION NAME(S) AND ADDRESS(ES)

Naval Research Laboratory
Oceanography Division
Stennis Space Center, MS 39529-5004

8. PERFORMING ORGANIZATION REPORT NUMBER

NRL/FR/7322--03-10,046

9. SPONSORING / MONITORING AGENCY NAME(S) AND ADDRESS(ES)

Office of Naval Research
800 North Quincy St.
Arlington, Virginia 22217-5560

10. SPONSOR / MONITOR'S ACRONYM(S)

ONR

11. SPONSOR / MONITOR'S REPORT NUMBER(S)

12. DISTRIBUTION / AVAILABILITY STATEMENT

Approved for public release; distribution is unlimited.

13. SUPPLEMENTARY NOTES
* Sverdrup Technologies, Inc., Stennis Space Center, MS 39529

14. ABSTRACT

Alongshore currents and nearshore dynamics generated on plane and barred beaches are successfully simulated using a shallow water model, ADCIRC, whose traditional applications have been focused on shelf-scale processes. ADCIRC-2DDI is a two-dimensional, finite-element-based coastal circulation model. Wave fields obtained from REF/DIF1, a monochromatic wave model that simulates refraction, diffraction, and wave breaking, are used to compute surface wave radiation stress gradients that force the hydrodynamic model. Processes such as advection, lateral diffusion/dispersion, and nonlinear bottom stress are examined at high resolution (~ 5 m) in order to determine their relative influence on the computed nearshore circulation. Unsteady circulation patterns are observed in our plane beach simulations for decreased values of the nonlinear bottom friction and/or lateral mixing coefficients. The structure and dynamics of these unsteady circulation patterns are very similar to shear waves described by Bowen and Holman (1989). Model-data comparisons made using data from Leadbetter, California (1980) and the 1990 DELILAH experiment at Duck, North Carolina, indicate that alongshore currents forced by wave radiation stress gradients are well simulated by the ADCIRC-2DDI model.

15. SUBJECT TERMS
Shelf-scale model   ADCIRC -2DDI   REF/DIF1

16. SECURITY CLASSIFICATION OF:			17. LIMITATION OF ABSTRACT	18. NUMBER OF PAGES	19a. NAME OF RESPONSIBLE PERSON
a. REPORT	**b. ABSTRACT**	**c. THIS PAGE**	UL	23	Cheryl Ann Blain
Unclassified	Unclassified	Unclassified			**19b. TELEPHONE NUMBER** *(include area code)* 228-688-5450

Standard Form 298 (Rev. 8-98)
Prescribed by ANSI Std. Z39.18

CONTENTS

APPLICATION OF A SHELF-SCALE MODEL TO WAVE-INDUCED CIRCULATION: ALONGSHORE CURRENTS ON PLANE AND BARRED BEACHES

1. INTRODUCTION

Wave-induced circulation is a typical feature of nearshore environments, and a more comprehensive predictive capability is essential for problems involving sediment and pollutant transport, water quality, or search and rescue operations. Several aspects of nearshore circulation are not well understood, such as the effect of advection, lateral and vertical mixing (diffusion/dispersion), and bottom boundary layer dissipation in regions of wave breaking (O'Connor and Yoo 1987; Svendsen and Putrevu 1994; Özkan-Haller and Kirby 1999). The purpose of this report is to establish the validity of using the ADvanced CIRCulation Model for Shelves, Coasts, and Estuaries – Two Dimensional, Depth-Integrated (ADCIRC-2DDI) shelf-scale hydrodynamic model in investigations of the dynamics associated with fine-scale wave-induced circulation. To achieve this goal, applications of the shelf-scale hydrodynamic model to nearshore environments in which the generation of alongshore currents is prominent are analyzed.

The shelf-scale numerical model under study is ADCIRC-2DDI (Luettich et al. 1992; Westerink et al. 1994a), a finite-element, two-dimensional barotropic hydrodynamic model. In the recent past, nearshore circulation models often have been limited in dynamical scope, including only wave-induced forcing mechanisms (e.g., Özkan-Haller and Kirby 1999; Van Dongeren and Svendsen 2000). One appealing aspect of the ADCIRC model is that it includes the full range of dynamical forcings (e.g., tides, wind, Coriolis effects, and river flux). More recent nearshore circulation models such as Delft3D (http://www.wldelft.nl/soft/d3d/index.html) address this issue but do not maintain the high degree of mesh flexibility afforded by the finite-element formulation of ADCIRC and its ability to simulate over nonuniform computational grids. Both the representation of shoreline geometric complexities and the placement of open ocean boundaries far from the coastal region of interest are easily handled using a single domain in the context of finite elements. Though ADCIRC has a successful history of modeling circulation associated with tides and storm surge, the successful applications of the ADCIRC model to fine-scale nearshore dynamics presented here are a first.

A series of ideal plane beaches provide a baseline for investigating the nearshore circulation of more complex bathymetries (Longuett-Higgins 1970a,b; Allen et al. 1996). Experiments over plane beaches are used to determine an appropriate configuration for the circulation model in terms of mesh resolution, boundary condition specification, and the sensitivity of the wave climate to model performance. The analysis includes a convergence study using Richardson-based error estimates (Blain et al. 1998) to define the grid resolution necessary to capture nearshore dynamics. Considerable emphasis is placed on understanding the sensitivity of nearshore circulation to variations in the nonlinear bottom friction and lateral mixing coefficients over ideal plane and barred beaches. In particular, time-dependent alongshore current behavior, similar in nature to shear waves studied by Bowen and Holman (1989), is examined in detail. The alongshore currents and nearshore circulation patterns generated by the shelf-scale dynamical model are scrutinized comprehensively against known and accepted circulation features reported in the literature.

In addition to the idealized settings, model-data comparisons are conducted using alongshore current observations obtained at two field sites. The first set of observations is from Leadbetter, California (a plane beach) on February 4, 1980 and the second set is the familiar Duck, North Carolina (a barred beach) set for the dates of October 7 and 13, 1990, taken as part of the DELILAH experiment. Application of the ADCIRC-2DDI model to the DELILAH beaches is an important test of the model since, unlike the ideal beaches examined, these beaches have longshore and cross-shore bathymetric variations that significantly increase the complexity of the circulation patterns.

The text that follows presents details describing the shelf-scale circulation model. The incorporation of wave effects through a surface wave radiation stress is discussed and the specifics of the wave simulator, REF/DIF1 (Kirby and Dalrymple 1994), that ultimately drives the circulation model, are also presented. Results for plane beaches are followed by barred beach applications.

2. ADCIRC-2DDI CIRCULATION MODEL

Sea surface elevation and coastal currents are modeled using the fully nonlinear, two-dimensional, barotropic hydrodynamic model ADCIRC-2DDI (Luettich et al. 1992; Westerink et al. 1994a). The ADCIRC model has a successful history of tidal and storm surge prediction in coastal waters and marginal seas (e.g., Blain et al. 1994; Kolar et al. 1994a; Westerink et al. 1994b; Blain et al. 1998) but prior to this work has not been applied to wave-driven flows. The basis of the ADCIRC-2DDI model is the depth-integrated shallow water equations, derived through vertical integration of the three-dimensional mass and momentum balance equations subject to the hydrostatic assumption and the Boussinesq approximation. To isolate processes associated with wave-driven nearshore flows, tidal, wind, and river forcing are neglected as well as Coriolis effects that tend to be minimal over small beach domains (~ 1 km). The resulting model equations include a continuity equation:

$$\frac{\partial \zeta}{\partial t} + \nabla_{xy} \cdot (H\nu) = 0, \tag{1}$$

and a momentum balance comprised of the local acceleration, advection and forcing through the barotropic pressure gradient, a surface wave stress, a bed stress, and lateral mixing, i.e.,

$$\frac{\partial \nu}{\partial t} + \nu \cdot \nabla_{xy}\nu = -\nabla_{xy}\left(g\zeta\right) + \frac{M_{xy}}{H} + \frac{\tau_{sxy}}{\rho_0 H} - \frac{\tau_{bxy}}{\rho_0 H}, \tag{2}$$

where *t* represents time, *x,y* are the Cartesian coordinate directions, ζ is the free surface elevation relative to the geoid, ν is the depth-averaged horizontal velocity vector, $H = \zeta + h$ is the total water column depth, *h* is the bathymetric depth relative to the geoid, *g* is the acceleration due to gravity, ρ_0 is the reference density of water, M_{xy} is the horizontal momentum diffusion/dispersion, τ_{sxy} are the applied horizontal free surface stresses, and τ_{bxy} are the horizontal bottom stress terms. This set of equations is considered to be time-averaged over a wave period. A spatially variable surface stress forcing is determined from the radiation stress ($S_{xx}, S_{yy}, S_{xy}, S_{yx}$) gradients of the wave field (Longuet-Higgins and Stewart 1964):

$$\tau_{sx} = -\left(\frac{\partial S_{xx}}{\partial x} + \frac{\partial S_{yx}}{\partial y}\right); \quad \tau_{sy} = -\left(\frac{\partial S_{yy}}{\partial y} + \frac{\partial S_{xy}}{\partial x}\right). \tag{3}$$

Bottom stress terms are parameterized using the standard nonlinear quadratic friction law:

$$\tau_{bxy} = C_f \rho_0 \left(u^2 + v^2 \right)^{1/2} v, \tag{4}$$

where C_f is the nonlinear bottom friction coefficient, and u,v are the x,y, components of velocity, respectively. Lateral mixing due to diffusion/dispersion is represented through the simplified eddy viscosity formulation of Kolar and Gray (1990):

$$M_{xy} = E_h \left(\nabla^2_{xy} (Hv) \right), \tag{5}$$

where E_h is the horizontal eddy viscosity coefficient for momentum diffusion/dispersion. The wetting and drying of computational elements is possible within ADCIRC-2DDI but is not used here. Preliminary simulations that allowed shoreline inundation indicated that for the beach profiles studied in this report, this process had negligible influence on the nearshore currents of interest. A rigorous derivation of the ADCIRC model equations is presented by Kolar et al. (1994b) and is not repeated here.

Numerical solution of the governing equations (Eqs. (1) and (2)) is achieved by recasting the continuity equation into a generalized wave continuity equation (GWCE) (Lynch and Gray 1979; Kinnmark 1984) and discretizing using the finite-element method, with the result that short wavelengths are successfully suppressed without resorting to nonphysical dissipation. The accuracy of this approach is well documented with respect to the solution of various shallow water problems (Lynch and Gray 1979; Luettich et al. 1992; Westerink et al. 1994a,c; Kolar et al. 1994a,b). The ADCIRC-2DDI hydrodynamic model solves the GWCE in conjunction with the momentum equations in nonconservative form.

3. INCORPORATION OF WAVE EFFECTS

The wave field used to force the ADCIRC-2DDI hydrodynamic model is derived from the linear, monochromatic wave model, REF/DIF1 (Kirby 1986; Kirby and Dalrymple 1994). The REF/DIF1 model is a phase-resolving, frequency domain model based on the parabolic approximation to the mild-slope equation for water wave propagation. Because REF/DIF1 is a monochromatic wave model in which a single wave frequency is propagated over irregular bathymetry, the wave-breaking region is narrower than what would be expected from a multispectral wave field. Regions of high wave-induced shear represent a significant test of the ADCIRC model's capability to simulate circulation that results from wave breaking in nearshore environments. REF/DIF1 uses a breaking criterion of $H > 0.78h$ (H is the wave height and h is the water depth) and a dissipation model to determine if wave breaking will occur (Kirby and Dalrymple 1994).

Wave heights and directions computed by the REF/DIF1 wave model are interpolated onto the nodes of the finite-element grid using a bicubic spline method. The radiation stress gradients are then computed for each element within the grid. Values are assigned to each node by averaging the radiation stress gradients of the surrounding elements. This averaging is necessitated by the inherent discontinuity of first derivatives (i.e., gradients) at the nodes when using linear triangle finite-element basis functions. It should be noted that gradients computed using a second-order finite difference approach yield essentially the same result and that use of an unstructured finite-element mesh results in no additional computational work.

In this study, REF/DIF1 and ADCIRC-2DDI are one-way coupled with the implication that the water elevations and currents determined from ADCIRC-2DDI do not affect the REF/DIF1 wave field during a simulation. The wave field as applied to the ADCIRC model is held constant for the duration of an experiment. Also neglected is the presence of wave orbital velocities that may alter the bottom shear

stress. Furthermore, all lateral mixing is represented by the momentum dispersion term M_{xy} previously discussed. No attempt is made to directly incorporate the mixing effects of waves through a spatially variable E_h (Thornton and Guza 1986; Özkan-Haller and Kirby 1999). A study by McDougal and Hudspeth (1986) indicates that the alongshore current profile of ideal plane beaches is rather insensitive to the parameterization of the lateral mixing and thus the exact form of this term is still open to debate. To summarize, wave effects are accounted for solely through a surface-wave stress gradient used as forcing for the ADCIRC circulation model.

4.   MODEL SENSITIVITY TO NEARSHORE CIRCULATION

One goal of this work is to determine an appropriate implementation in nearshore environments for the ADCIRC model that is traditionally applied to shelf-scale hydrodynamics. Issues considered include mesh resolution, model configuration including the lateral boundary condition and model time step, and the effect of the initial wave climate on computations.

4.1 Mesh Resolution

A grid convergence study is conducted to determine the resolution necessary to capture wave-driven circulation. Wave breaking leads to sharply discontinuous radiation stress gradients and represents a significant test of the ability of the ADCIRC model to simulate wave-induced nearshore circulation. A coarse resolution mesh will tend to artificially smooth the wave height field and ultimately reduce the associated radiation stress gradients in the wave-breaking region. In contrast, a very fine mesh (i.e., one that is equal to or greater than the resolution of the wave field) risks resolving very large radiation stress gradients over very small regions of the mesh. Such a situation could result in unstable computations or, in turn, might require unrealistically high lateral mixing and/or dissipation to obtain a stable solution.

We apply a Richardson-based error estimation (Roach 1994; Blain et al. 1998) to determine if the nodal resolution of the simulations produces converged solutions of the alongshore current. The Richardson-based error estimates for a grid of specified resolution are derived through a comparison of the computed solution over that mesh with the solution computed over either a coarse grid (a grid having *half* the resolution of the select grid) or a fine grid (a grid having *double* the resolution of the select grid). Convergence results when the coarse and fine grid error estimators are approximately equal indicating errors are in the asymptotic range, i.e., the solution over that grid will not change by using a finer grid resolution. Typically, absolute convergence is quite difficult to achieve due to computational limits and/or numerical truncation errors produced by the model itself.

For an ideal plane beach (slope = 0.009) discretized using three uniform grid resolutions of 10 m (7701 nodes), 5 m (30,401 nodes), and 2.5 m (120,801 nodes), the maximum values for coarse and fine grid error estimates differ by approximately a factor of 2 (not shown). However, for the majority of nodes (585 –70%), the fine grid/coarse grid elevation differences are centered about zero. Furthermore, the distribution of error over the grid changes little in comparing the 5-m grid solution to either the 10-m or 2.5-m grid solutions. Thus, errors associated with the 5-m grid are considered close to the asymptotic range such that convergence of the 5-m grid solution is assumed. As such, any errors due to grid resolution are at a minimum. Based on this analysis, a 5-m grid resolution is considered to be suitable to capture the dynamics associated with circulation in the nearshore environments modeled here (i.e., alongshore currents). The uniform finite-element mesh constructed to represent the plane beach resolved with 5-m nodal spacing requires 60,000 elements and 30,401 nodes. This mesh is used for all remaining plane beach simulations presented.

4.2 Model Configuration

A radiation condition applied at the lateral boundaries yields the most realistic nearshore circulation patterns, as opposed to the no flow lateral boundary condition, by allowing flow to exit the domain in the alongshore direction. The radiation condition permits a flux per unit width of boundary q to exit the domain through the lateral boundary. This flux is defined by the product free surface departure times the speed of a gravity wave (e.g., $q = \sqrt{gh}\eta$). Sensitivity of the computed nearshore circulation to the model time step is investigated by comparing model simulations having time steps of 0.25 s and 0.125 s. No measurable difference in the computed solutions is observed. As long as the Courant condition (Westerink et al. 1994a) is satisfied, the nearshore circulation is not sensitive to the time step of the simulation.

4.3 Wave Climate

The model configuration outlined above (i.e., 5-m resolution, radiation lateral boundaries, and 0.25-s time step) for plane beaches is now applied to beaches that vary in slope (0.006 and 0.009), minimum depth (0.1 m and 1.6 m), and incident wave conditions (5-s and 10-s periods, 1.0-m and 2.0-m heights, and 5-deg and 30-deg direction), to validate robustness of the model for nearshore computations. The following observations are made from the simulated current fields: 1) cross-shore water elevation profiles are relatively insensitive to the incident wave direction and period, and 2) the magnitude of the alongshore current depends quite strongly on the incident angle and weakly on the wave period. The ADCIRC model-simulated alongshore current profiles exhibit single peaks coincident with the location of wave breaking that is typical of plane beaches (Longuet-Higgins 1970b).

5.   SENSITIVITY OF THE ALONGSHORE CURRENT ON PLANE BEACHES

In order to understand the effects of nonlinear bottom friction and lateral mixing on nearshore sea surface elevation and alongshore currents, the 0.009 slope plane beach, with a wave period of 10.0 s, incident wave direction equal 30 deg, and an incident wave height of 1.0 m is simulated using several different values for the coefficients of friction and eddy viscosity (Fig. 1). The range of values selected for the friction coefficient C_f is of the same order of magnitude as those obtained in previous studies of actual plane and barred beaches (Church and Thornton 1993; Whitford and Thornton 1996). In an analogous way, the values of E_h used here are of the same order of magnitude as those presented in a recent study using a similar lateral mixing formulation for comparable waves fields and bathymetry (Özkan-Haller and Kirby 1999). Admittedly though, the lack of field data makes it far more difficult to determine an appropriate range of values for E_h.

5.1 Steady Circulation

The cross-shore mean water level (not shown) is relatively unaffected by changes in the coefficients of friction and eddy viscosity. This insensitivity of the cross-shore water elevation is expected since mean water levels in the cross-shore direction result primarily from a balance of the cross-shore forces, i.e., the radiation stress gradient and pressure gradient that is only weakly dependent on the circulation.

On the contrary, the alongshore current is found to be very sensitive to the coefficients of friction and eddy viscosity. Recall that friction and lateral mixing are dissipative and diffusive effects that depend strongly on the generated velocity. Increasing the nonlinear bottom friction coefficient decreases both the peak alongshore current and the magnitude of the alongshore current in the region shoreward of breaking.
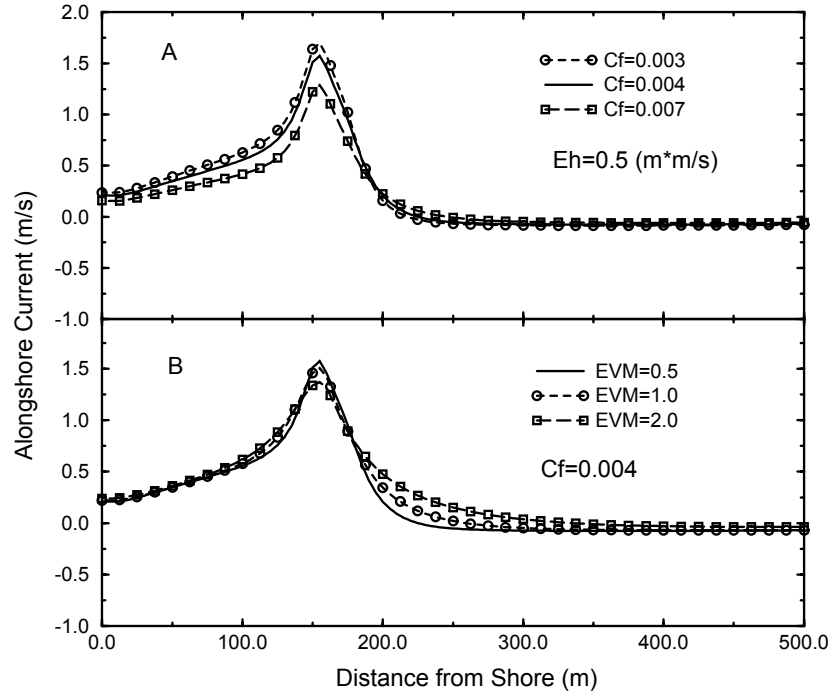
Fig. 1 — Alongshore current sensitivity to bottom friction and eddy viscosity coefficients for the ideal plane beach (slope = 0.009, wave period = 10.0 s, incident wave direction = 30 deg, incident wave height = 1.0 m) along a cross-shore transect at 750 m. (A) Alongshore current (m/s) for E_h = 0.5 m^2/s, C_f = 0.003, 0.004, 0.007 and (B) Alongshore current (m/s) for C_f = 0.004, E_h = 0.5, 1.0, 2.0 m^2/s.

The shape of the alongshore current profile remains unaffected (Fig. 1(A)). Increasing the lateral mixing coefficient E_h also leads to a reduction of the peak alongshore current but to a much lesser degree. Larger values of E_h tend to smooth the alongshore current profile by increasing the diffusion and dispersion of alongshore momentum in the cross-shore directions (Fig. 1(B)). Note the offshore alongshore current that is directed opposite to the peak alongshore current. The magnitude of this opposing current decreases slightly as dissipation or lateral mixing is decreased.

5.2 Unsteady Circulation

Alongshore current shear instabilities or shear waves have been observed in prior computational and experimental studies of plane and barred beaches (e.g., Bowen and Holman 1989; Dodd et al. 1992; Allen et al. 1996). The complex unsteady dynamics of shear instabilities provide a challenging test for the ADCIRC model as a simulator of nearshore dynamics. Commonly, nearshore shear instabilities are generated in the vicinity of the wave-breaking region when the alongshore current becomes unsteady. Such shear instabilities can result in the generation of a shear wave that propagates in the direction of the alongshore current.

The emerging picture of shear waves suggests that they could be a significant mechanism of nearshore lateral mixing (Putrevu and Svendsen 1992) in the vicinity of wave breaking. If shear waves are an important mechanism of lateral mixing, then their appearance in a nearshore simulation would be determined, at least to some degree, by the strength of the lateral mixing term. Previous studies (Allen et al. 1996; Slinn et al. 1998) clearly demonstrate that shear waves are sensitive to increasing dissipative effects through the bottom friction. Clearly then, the magnitudes of the lateral mixing and bottom friction terms within the ADCIRC model are expected to significantly affect the generation of shear waves.

Shear wave circulation patterns are observed on the plane beach (same initial wave conditions as above) when nonlinear bottom friction and/or lateral mixing coefficients are decreased below some threshold values, e.g., $C_f < 0.003$ and $E_h < 0.3$ m^2/s for a slope of 0.009. Recall from Fig. 1 that a reduction in dissipation or lateral mixing leads to increased magnitudes of the alongshore velocities both nearshore and offshore. This increase results in a larger cross-shore gradient of the alongshore velocity and a subsequent steepening of the alongshore current profile. When the alongshore current shear becomes very large, vortex generation occurs.

Using the 0.009 ideal plane beach, the computed currents are examined when C_f is lowered to a value of 0.002 and $E_h = 0.5$ m^2/s. Unsteady vortices appear in the circulation pattern and propagate in the direction of the alongshore current (Fig. 2(a)). These vortices result in localized regions of set-down in the mean sea level seaward of the alongshore current as seen from Fig. 2(a). Vortices form in the domain at the first occurrence of wave breaking and grow in magnitude as they propagate in the alongshore direction. For this particular case, the vortices are fully developed after traveling approximately 750 m in the alongshore direction. Additionally, set-up of the mean sea level shoreward of the alongshore current changes in response to the vortex motion. Figure 3 shows the velocity field of a single vortex, delineated in Fig. 2(a). It should be noted that the maximum set-down (Fig. 2(a)) does not occur in the center of the vortex, but rather between the vortex center and the peak alongshore current where the alongshore current and vortex circulation are coincident (Fig. 3). The maximum set-down in these regions is approximately two to three times greater than the steady state set-down. Figure 4 shows the steady state case represented by $C_f = 0.004$, $E_h = 0.25$ m^2/s. The computed velocity field is also quite similar to the shear wave velocity field predicted for a beach of constant horizontal bathymetry (Bowen and Holman 1989).

Contours of the vorticity field (s^{-1}) associated with the nearshore circulation are shown in Fig. 2(b) and correspond directly to the mean sea level depicted in Fig. 2(a). From Fig. 2(b) it is apparent that vorticity of opposite sign (clockwise and counterclockwise) occurs at onset of wavebreaking and propagates in the alongshore direction. The alongshore current generates a strong velocity shear that creates vortex-like structures when the dissipation or lateral mixing is weak enough to allow it. These vorticity patterns are similar to those obtained by Allen et al. (1996) and Özkan-Haller and Kirby (1999) for ideal plane beaches. Closed vortices form only on the seaward side of the alongshore current (Fig. 2(b); Fig. 3). On the shoreward side, currents with clockwise orientation are generated but a closed vortex does not form. The most likely explanation for the absence of complete vortex formation on the shoreward side is a weaker current shear.

Bowen and Holman (1989) find that shear waves have approximate celerities between 1/3 V_{max} to V_{max}, where V_{max} is the maximum alongshore current velocity, frequencies are on the order of 10^{-3} to 10^{-2} Hz, and wavelengths are approximately $2\Delta x$, where Δx is the cross-shore width of the alongshore current peak. For the plane beach with slope 0.009, $C_f = 0.002$, and $E_h = 0.5$ m^2/s, the frequency of the observed vortices is approximately 0.003 Hz (see Fig. 4) and the separation of the vortices is about 230 m (Fig. 5). The value of Δx is estimated to be 100 m based on the distance between vortex pairs, and the celerity of the vortices is approximately 0.6 to 0.69 m/s. Similar estimates of shear wave characteristics are obtained for the plane beach simulation using values of $C_f = 0.004$, and $E_h = 0.25$ m^2/s (see Figs. 4 and 5). Clearly, the frequency, wavelength, and celerity values of the unsteady circulation computed from ADCIRC model solutions are well within the predicted range for shear waves.
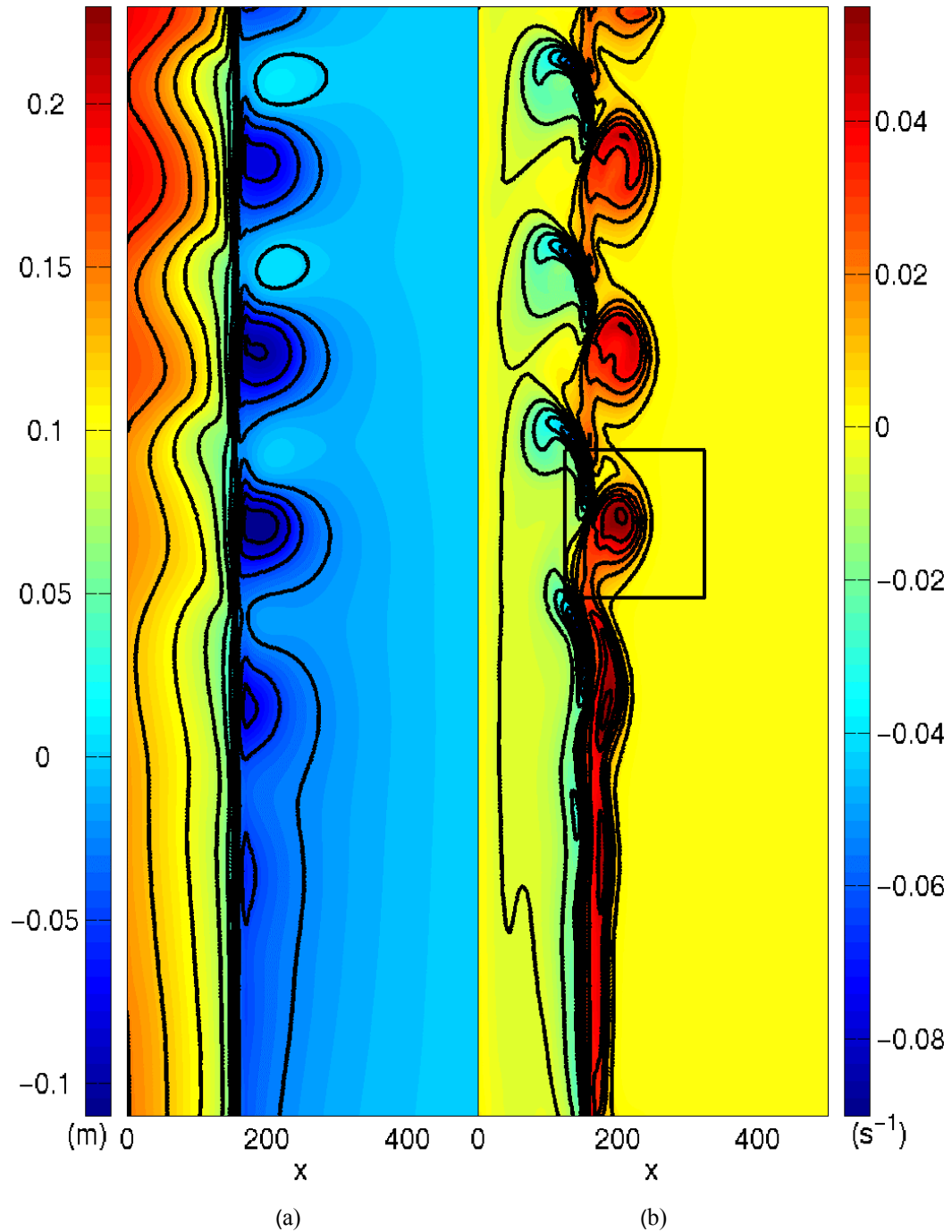
Fig. 2 — Unsteady circulation on an ideal plane beach (slope = 0.009, C_f = 0.002, E_h = 0.5 m^2/s); a) sea surface elevation (m) and b) vorticity (s^{-1}). The shoreline is on the left and the alongshore current is moving upward, with respect to the page, in a positive Y direction.
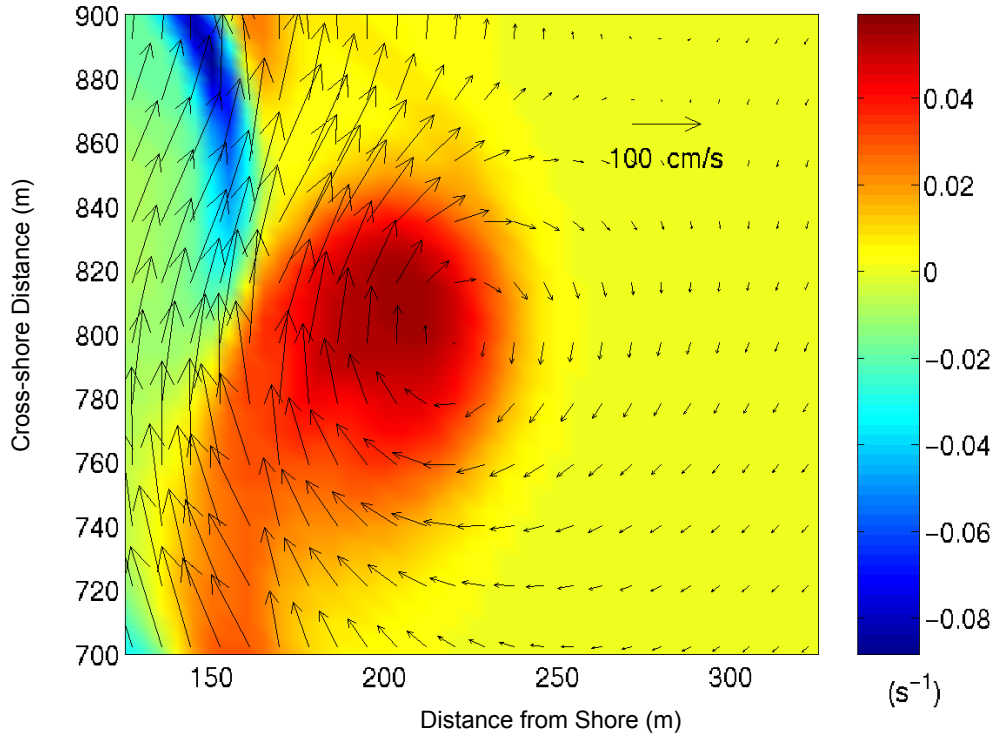
Fig. 3 — Unsteady circulation on an ideal plane beach (slope = 0.009, C_f = 0.002, E_h = 0.5 m²/s). Vorticity (filled) and velocity vectors (m/s) magnified from the boxed region in Fig. 2a. The maximum alongshore current is located ~150 m offshore.
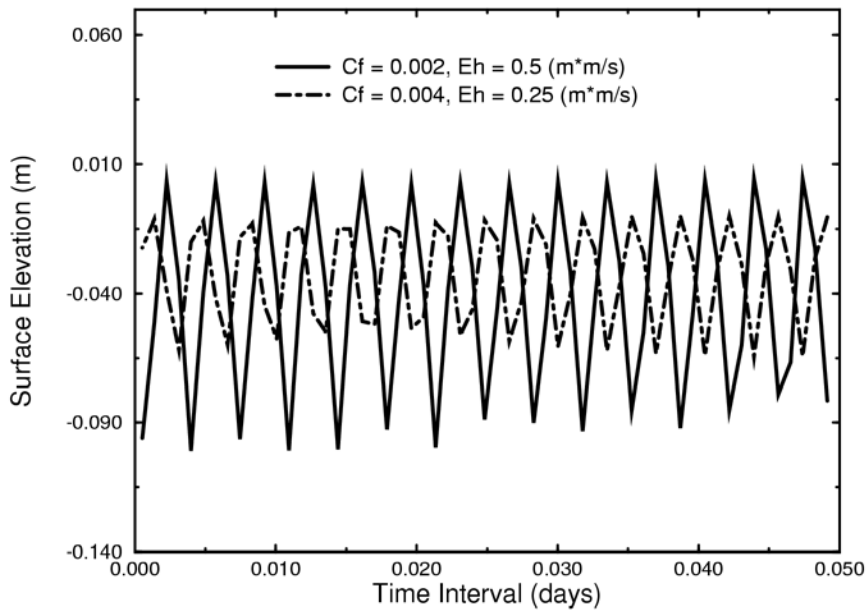

Fig. 4 — Vortex frequency for the unsteady ideal plane beach. Shown are alongshore surface elevations (m) for the steady (C_f = 0.002, E_h = 0.5 m²/s — solid line) and unsteady (C_f = 0.004, E_h = 0.25 m²/s — dot-dashed line) states at 210 m offshore and 750 m alongshore.
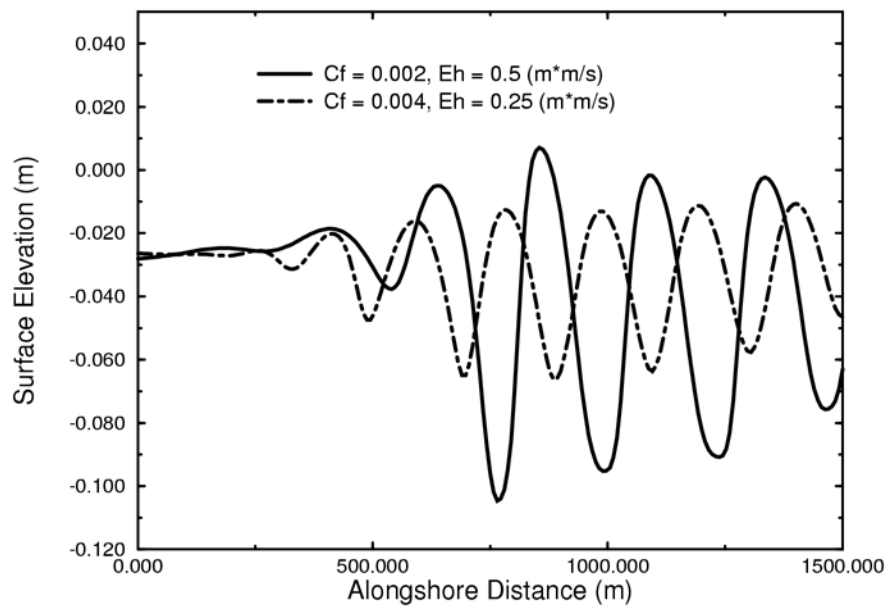
Fig. 5 — Vortex separation distance for the unsteady ideal plane beach. Shown are alongshore surface elevations (m) for $C_f = 0.002$, $E_h = 0.5$ m^2/s (solid line) and $C_f = 0.004$, $E_h = 0.25$ m^2/s (dot-dashed line) at 210 m offshore and 750 m alongshore.

The time-dependent states that appear on the plane beach are completely stable and cycle periodically as a larger-scale circulation pattern for the duration of the simulation. To be assured that the unsteady circulation is not merely a numerically excited, long-lived transient mode and to test the robustness of the observed shear waves, Gaussian noise is introduced into the radiation stress field. If the shear wave circulation pattern is a stable mode of the system, it should persist even when subject to random fluctuations in the radiation stress forcing. Gaussian noise is added to the steady radiation stress field such that the maximum deviation of the radiation stress field at any point from its original value is 5.0%. This level of noise does not significantly alter the computed unsteady circulation pattern. In fact, the resulting circulation is essentially identical to the unperturbed circulation pattern. As a further test, the radiation stress forcing is perturbed in time within a given simulation. This action results in more noticeable alterations of the current field. Namely, vortex formation occurs further downstream in the alongshore direction, essentially damping the onset of shear wave generation. Nevertheless, in time, the overall shear wave circulation pattern persists.

Previous studies have successfully used periodic boundary conditions (e.g., Allen et al. 1996; Özkan-Haller and Kirby 1999) to model shear waves, and questions have been raised as to the role periodic boundary forcing plays in the generation of periodic vortex structures. The use here of a radiation boundary condition along lateral boundaries offers a more realistic representation of the dynamics associated with nearshore beaches and does not inhibit the formation of shear waves. The quantification of any errors associated with the use of a radiation condition is left for further study.

6. A FIELD CASE: LEADBETTER BEACH, CALIFORNIA

The site of a field study, Leadbetter, California (Thornton and Guza 1986) is simulated for the time period of February 4, 1980. Leadbetter beach is essentially planar, flat to within about 85 m of the shore

and sloping upwards toward the shoreline at an incline of approximately 0.04. The discrete representation of Leadbetter beach has dimensions of 185 m by 200 m (cross-shore by alongshore) and a nodal spacing of approximately 6.0 m, requiring a mesh of 2048 elements and 1089 nodes. The wave field at Leadbetter beach is characterized by an incident wave height of 0.56 m, an incident direction of 9.0 deg, and a wave period of 14.2 s. Each simulation was run for 14.4 hours with a time step of 0.25 s.

Both wave height and alongshore current magnitude are measured over a transect that runs from nearshore to offshore. Observed alongshore currents are compared with modeled alongshore currents to determine the influence of advection, nonlinear bottom friction, and lateral mixing. For February 4, 1980, Leadbetter field observations and REF/DIF1 computed wave heights at the same location (Fig. 6(B)) agree reasonably well within the nearshore region (< 84 m offshore). REF/DIF1 is a suitable wave model for this scenario since the observed wave spectrum is known to be narrow-banded in frequency and direction.

In Fig. 6(C), the measured alongshore current data from Leadbetter are compared against two computed profiles of the alongshore current using parameter values of $C_f = 0.006$ and $E_h = 0.5$ m^2/s. The values for C_f and E_h were chosen to minimize the difference between the calculated and observed alongshore current peak. The sensitivity of the alongshore current profile to changes in these parameters is similar to that shown in Fig. 1. Figure 6(C) presents computations that include and exclude material derivative terms, i.e., advective plus local acceleration terms. Since computations undertaken are run to a steady state, local acceleration terms essentially vanish and the role of advection on the alongshore current profile can be considered. From Fig. 6(C), the exclusion of advection results in a better agreement between the computed and observed peak alongshore current. The inclusion of advection damps the peak alongshore current and shifts it shoreward. Offshore, the alongshore current computed by including advective processes has magnitudes that are in better agreement with observations but do not decrease with increasing offshore distance. The primary difference between the ideal plane beach considered previously and Leadbetter beach is the steepening slope from near 75 m to the shore (Fig. 6(A)). This change in the bathymetric gradient is not accompanied by additional mesh resolution. Advective processes are known to be quite sensitive to the representation of velocity gradients (Hench and Luettich 1998) and for this case such gradients may not be well represented. Additionally, the effect of such bathymetric transitions on enlarging the truncation error of the numerical solution has recently been reported by Hagen et al. (2000) in the context of one-dimensional tidal simulations. Since advection is not regarded as a dominant process in the generation of alongshore currents, further investigation of the relation between advective processes and grid resolution is left for future studies.

Dodd et al. (1992) reported that shear wave states might have been observed in the February 4, 1980 Leadbetter data but the existence of such states could not be determined conclusively. The possibility of shear instabilities at Leadbetter beach, based on the bathymetry of February 4, 1980, is now investigated. The expected wavelengths for shear instabilities (Bowen and Holman 1989) are approximately twice the cross-shore width of the peak alongshore current region, or approximately 100 m for Leadbetter beach. In order for a shear wave mode to fully develop, the alongshore length of the domain should be about 600 m to 750 m, based on the results of the ideal plane beach. Thus, the initial domain length of 200 m is extended to 1400 m in the alongshore direction. A parameter study is performed in which the nonlinear bottom friction and eddy viscosity coefficients are made progressively smaller in order to observe a transition from steady to unsteady circulation. Although the existence of shear waves or unsteady states at Leadbetter beach cannot be ruled out, the generation of unsteady states in the ADCIRC model simulations of Leadbetter beach was not observed.
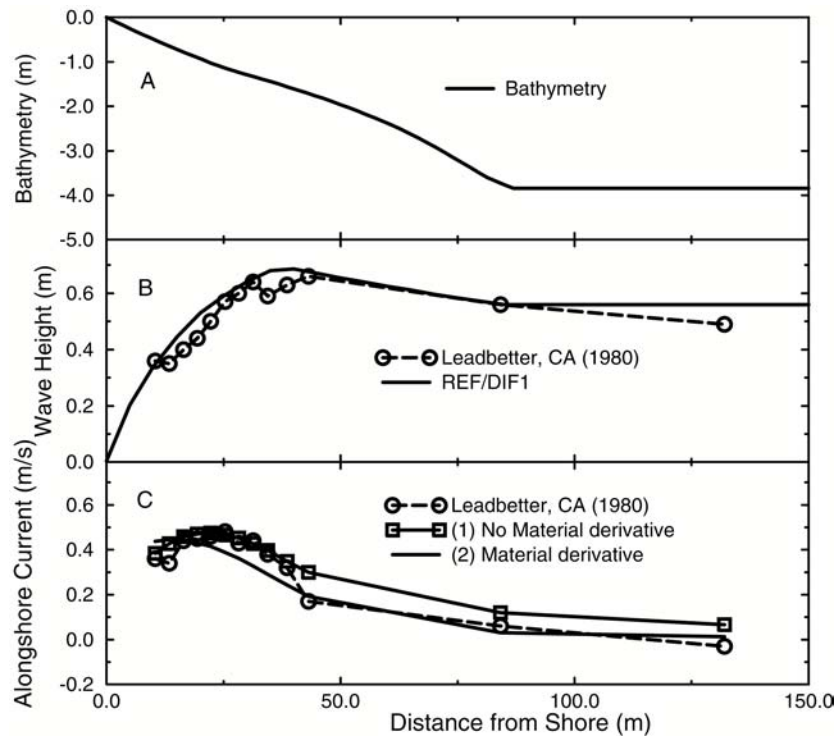
Fig. 6 — Leadbetter beach, CA (1980) along a cross-shore transect at 100 m; (A) Bathymetry; (B) Measured wave heights (circles) and REF/DIF1-computed wave heights (solid line); and (C) Measured alongshore current (circles), with (1) no material derivative terms (squares), and (2) material derivative terms included (solid line).

7. LONGSHORE CURRENTS ON BARRED BEACHES

The barred beach represents a common bathymetry found in nearshore environments and one that has been studied extensively in previous works (e.g., Ebersole and Dalrymple 1980; Putrevu and Svendsen 1992; Slinn et al. 1998; Lippmann et al. 1999; Özkan-Haller and Kirby 1999). The DELILAH field experiment of the barred beach at Duck, North Carolina, in 1980 finds a strong alongshore current peak in the bar trough whereas modeling studies produce alongshore current profiles with two peaks, one on the bar crest and another near the shoreline (e.g., Garcez Faria et al. 1996; Slinn et al. 1998). The barred beach offers yet another test for the ADCIRC model as a simulator of nearshore environments.

7.1 Ideal Barred Beach

The ideal barred beach examined (Fig. 7(A)) is an approximate representation of the bathymetry measured on October 11, 1990 at Duck, North Carolina, as part of the DELILAH experiment (e.g., Slinn et al. 1998); note, however, that the bathymetry for this idealized case is symmetric in the alongshore direction. The ideal barred beach is plane with an offshore slope of approximately 0.007 and a bar located 80 m from the shoreline. The simulation parameters for the ideal barred beach are identical to those of the steady ideal plane beach: $C_f = 0.004$, $E_h = 0.5$ m^2/s. The incoming wave is specified to have a height and direction of 1.4 m and 20 deg, respectively, and a wave period equal to 8.0 s. As shown by Figs. 7(B) and (C), strong wave breaking occurs 90 m offshore on the outer flank of the bar crest and again approximately 15 m offshore on the foreshore, shoreward of the bar trough. The result is two peaks in the

alongshore current (Fig. 7(C)) coincident with the locations of wave breaking. The alongshore current associated with primary wave breaking corresponds well to the location of the observed alongshore current peak at low-tide or mid-tide conditions (Thornton and Kim 1993). The low-tide/mid-tide scenarios are more consistent with the zero tidal offset prescribed for the wave model. The secondary peak in the alongshore current produced by the ADCIRC model is not evident in the field data. This simulated two-peak structure of the alongshore current is also obtained by other models of idealized barred beaches, e.g., Thornton and Kim (1993) and Slinn et al. (1998), indicating that cross-shore bathymetric variations play perhaps an important role in the generation of the alongshore current. While the magnitude of the alongshore current predicted by ADCIRC is remarkably similar to the values presented by Slinn et al. (1998), it is slightly overpredicted in comparison to the observations.
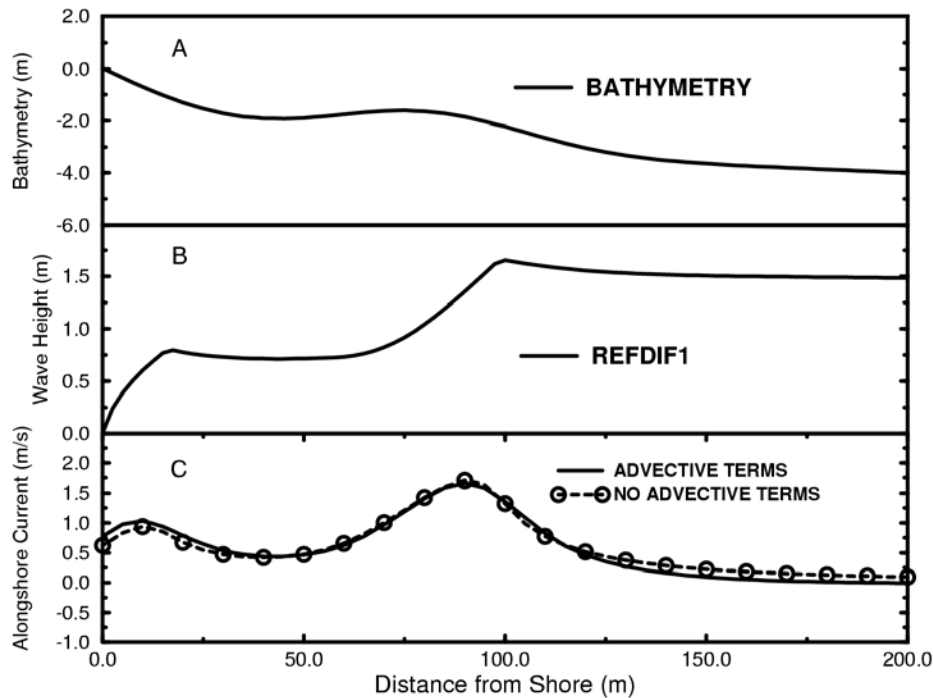

Fig. 7 — Ideal barred beach along a cross-shore transect at 200 m; a) bathymetry, b) REF/DIF1 wave heights (m), and c) ADCIRC alongshore current (m/s) computed with (solid line) and without (dashed line with circles) advective terms.

In order to obtain both primary and secondary wave breaking (as observed in the field, e.g., Thornton and Kim 1993) using the monochromatic wave model REFDIF1, an incident wave height of 1.4 m is used. Note that this value for the incident wave height is nearly twice that used by Slinn et al. (1998) in their spectral wave representation. However, at 200 m offshore, the 1.4-m incident wave height compares well to the observed wave height of approximately 1.2 m. This ideal barred beach application serves as a baseline for understanding and interpreting the alongshore current profiles over more complex bathymetry.

7.2 A Field Case: Duck, North Carolina

The Duck, North Carolina, beach bathymetry measured during the 1990 DELILAH experiment represents a realistic and complex environment for the prediction of nearshore currents. The bathymetries

for October 7 and 13 vary considerably in the alongshore direction unlike the ideal barred beach just examined. Figure 8 shows the October 13 bathymetry contours. The alongshore profiles in Fig. 9 represent the bathymetry at locations where alongshore current data is recorded for the DELILAH experiment. The primary difference between the October 7 and 13 bathymetries is their bar and trough structure. These bathymetric variations provide additional insight into how such features influence formation of the alongshore current.
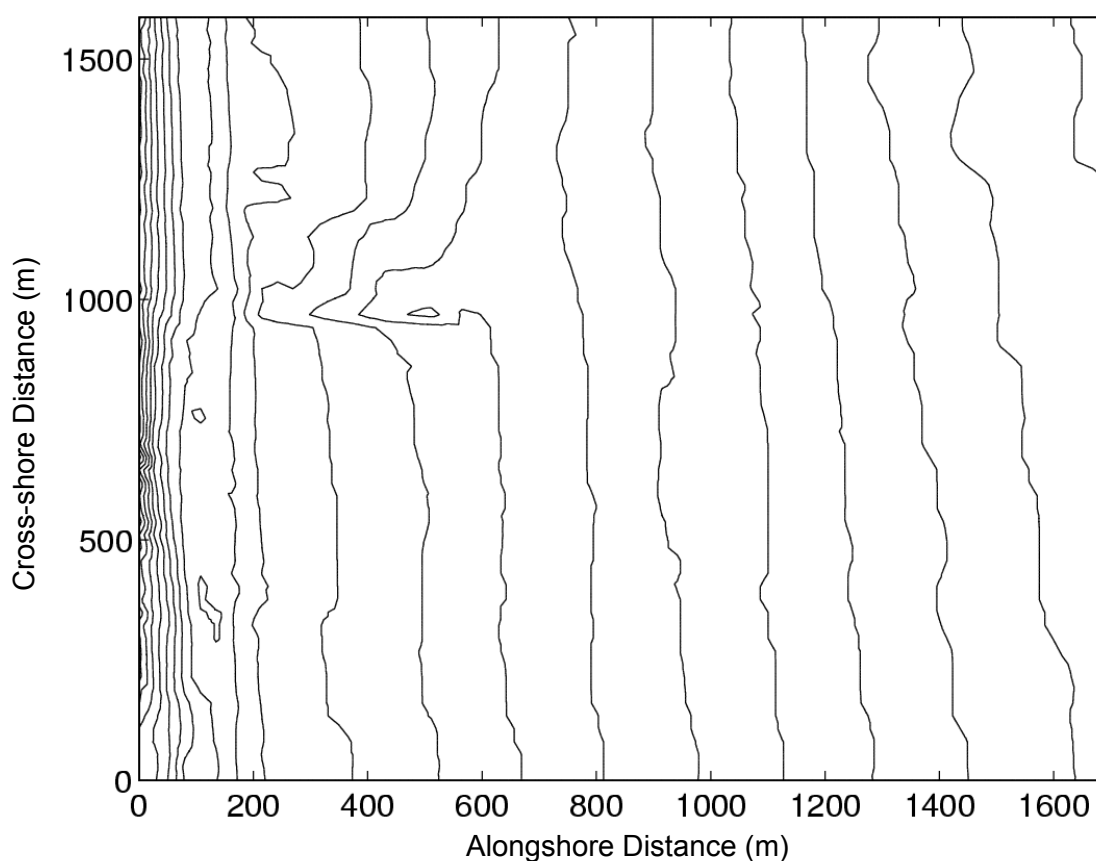

Fig. 8 — Bathymetry contours from the October 13, 1990 DELILAH experiment at Duck, NC. The shoreline is located to the left.

The model domain for the Duck simulations has dimensions of 1695 m cross-shore by 1587 m alongshore, and is discretized to a level of 6.72 m, using 118,944 elements and 59,961 nodes. The offshore slope in the bathymetry, along the cross-shore array, is approximately 0.007. A cross-shore array with nine data recording stations provides field measurements of the alongshore current and wave height (Fig. 9). Low wind speeds and a relatively low occurrence of bad data prompted selection of the October 7 and 13 dates. Note, however, that the alongshore current data taken October 7 at 68 m and October 13 at 68 and 169 m are not used due to their obviously poor quality. Additionally, there are no wave height data for October 13 at 169 m.

The REF/DIF1 computed wave field for October 7 (October 13) is generated from an incident wave height of 0.53 m (2.38 m), an incident wave direction of -28.0 deg (-26.0 deg), a wave period of 10.72 s

(11.976 s), and a tidal offset of –0.246 m (0.671 m); these values are derived from the observed wave fields. In order to make realistic model-data comparisons, mean tidal offsets in water depth are accounted for in the calculation of the wave field. Note that all subsequent mean values, i.e., tidal variations of water depth, wave height, and alongshore currents, are determined by averaging over the 2 h and 16 min sampling window of each set of data.
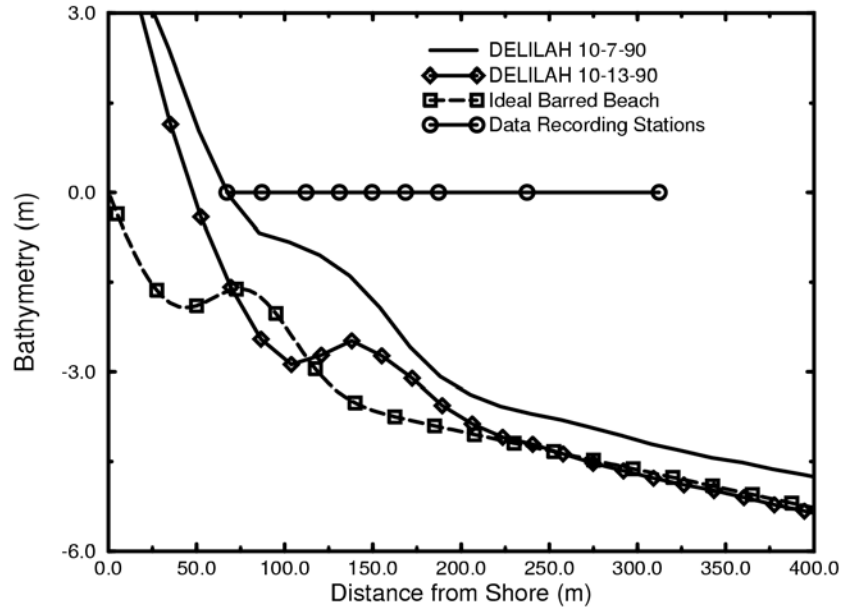

Fig. 9 — Barred beach experiments. Bathymetry for DELILAH October 7 (solid line) and October 13, 1990 (diamonds), the location of the nine cross-shore array recording stations (circles), and the ideal barred beach bathymetry (squares).

Comparisons between mean values of the wave height measurements on October 7 and 13 and the modeled REF/DIF1 wave heights are shown in Figs. 10(A) and 11(A), respectively. For the purposes of this study, the observed and modeled wave heights are in reasonably good agreement. The over-prediction of the simulated wave heights prior to wave breaking for both time periods can be attributed to the monochromatic nature of the REF/DIF1 model.

In Fig. 10(B), the October 7 ADCIRC computed alongshore current using values of $C_f = 0.008$ and $E_h = 0.5$ m^2/s is plotted against the maximum, minimum, and mean observed alongshore current. Advective processes are not included for these calculations. The alongshore current profile from ADCIRC represents fairly well what is observed given the limitations of the computed wave field. Underprediction of the offshore values of the alongshore current can be linked directly to discrepancies between the measured and computed wave height offshore. Deviation of the nearshore alongshore current from observed values at the same location can also be attributed to the presence of secondary wave breaking at approximately 75 m offshore.

The model-data comparisons for the ADCIRC alongshore current against the October 13 data ($C_f = 0.008$ and $E_h = 1.0$ m^2/s) are presented in Fig. 11(B). For the October 13 bathymetry, it is necessary to use a greater value of the lateral mixing coefficient, E_h, to achieve a reasonable solution, a consequence perhaps of the greater cross-shore bathymetric variability. Agreement between the simulated and observed alongshore current is much worse for October 13. The REF/DIF1 wave heights exhibit distinct

regions of primary and secondary breaking much like for the ideal barred beach. Consequently, the computed alongshore current has a strong peak on the offshore bar face at the location of primary breaking. Observed wave heights do not exhibit such distinct regions of breaking resulting in a smoothly varying alongshore current profile that lacks a distinct peak structure. From Fig. 11(B), the inclusion of advection reduces the magnitude of the peak alongshore current and shifts its occurrence shoreward towards the bar crest. This influence of the advective terms is similar to that described at Leadbetter beach. The influence of advective processes appear quite sensitive to the resolution of bathymetric features including sharp transitions in slope and/or the cross-shore and alongshore variability. From these applications of the ADCIRC model to wave-induced flow during the DELILAH experiment, the sensitivity of the alongshore current to the representation of wave height is obvious and not surprising since the sole driving force for these currents is the radiation stress gradients. Expectations are that a spectral representation of the wave field may improve comparisons between computed and measured alongshore currents. Overall the ADCIRC model reproduces the general trends of the alongshore currents in both field data sets quite well.
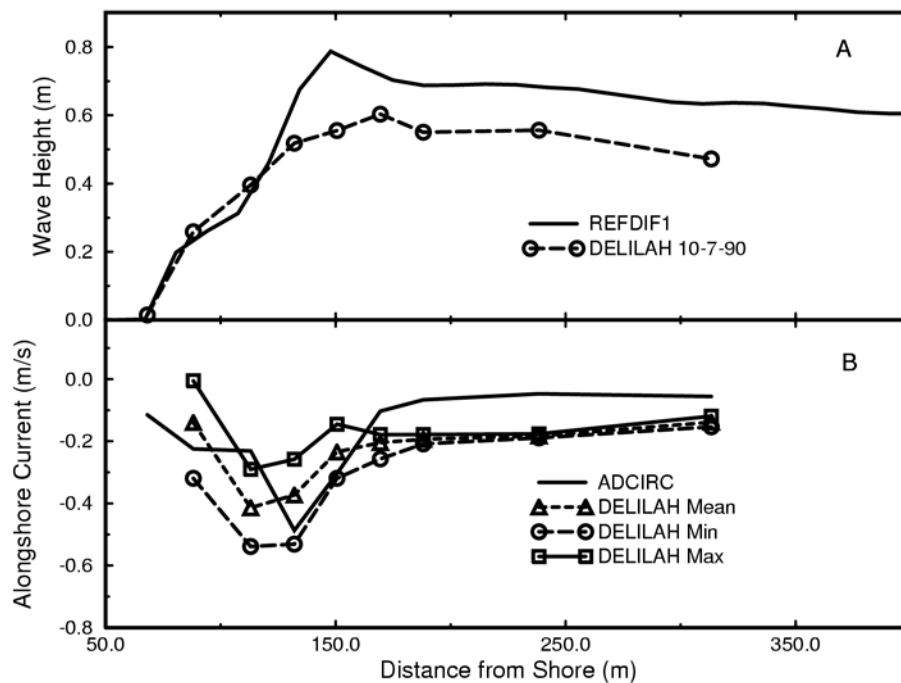

Fig. 10 — Duck, NC October 7, 1990, 0400-1616 hr; (A) mean observed wave heights (circles) compared to REF/DIF1 computed wave heights (solid line) and (B) computed (solid line) and max. (squares), min.(circles), and mean (triangles) observed alongshore current. Model computations are sampled at observational locations.
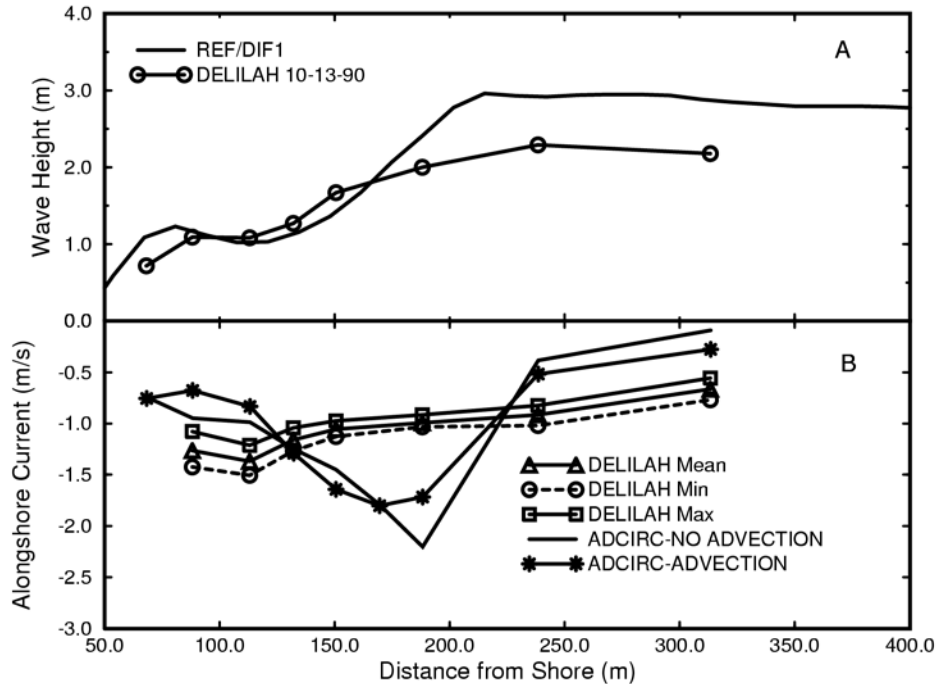
Fig. 11 — Duck, NC October 13, 1990, 0100-0316 hr; (A) mean observed wave heights (circles) compared to REF/DIF1 computed wave heights (solid line) and (B) alongshore current computed without advection (solid line), with advection (stars), and the max. (squares), min. (circles), and mean (triangles) of the observed alongshore current.

8. CONCLUSIONS

The purpose of this study has been to determine if a traditionally shelf-scale hydrodynamic model, such as ADCIRC, can be successfully applied in nearshore environments and if so, to understand the sensitivities of the model to processes relevant to nearshore dynamics. The analysis of alongshore currents generated on plane and barred beaches, both ideal and field cases, clearly indicate that the ADCIRC model produces physically realistic nearshore circulations.

Successful application of the ADCIRC model to plane beaches at converged resolutions of 5 m is a first. Computed mean sea levels and circulation patterns resulting from small-scale, wave-driven dynamics compare well with what is known and reported in the literature. Additionally, the ADCIRC model reproduces the respective alongshore current profiles of several field experiments (Leadbetter Beach and Duck, NC) reasonably well. The sensitivity of the alongshore current to magnitudes of the bottom friction and lateral mixing terms provide insight into the relative importance of lateral and vertical mixing and bottom dissipation in a wave-breaking regime. Decreases in the nonlinear bottom friction and/or lateral mixing coefficient results in a transition from steady to unsteady circulation. As such, it is possible to simulate complex time-dependent behavior such as shear waves (Bowen and Holman 1989). The shear waves generated are well-predicted in terms of the parameters established to define such waves in the nearshore. Model-data comparisons to field observations taken at Leadbetter (1980) and Duck as part of the 1990 DELILAH experiment clearly show that ADCIRC-2DDI is capable of modeling alongshore currents and the nearshore circulation features of real beaches.

Lastly, the role of advection in computations at Leadbetter beach and Duck demonstrate the sensitivity of advective processes to complexities in the bathymetry such as sharp changes in gradient or

cross-shore variability. Over smooth bathymetric profiles such as those prescribed for the ideal plane and barred beaches, advection is clearly not a dominant process in the generation of alongshore currents. Future studies will address the relation between advection, the resolution of bathymetric features, and the generation of alongshore currents.

It should be emphasized that application of the shelf-scale model ADCIRC to nearshore problems has several advantages. First, the model contains the full suite of nonlinear dynamical forcings such as tides, wind, and Coriolis acceleration so that the entire range of coastal ocean processes can be considered in nearshore environments. (More recent versions of the ADCIRC model also include the effects of density gradients.) Secondly, the finite-element formulation and its use of unstructured grids allow considerable flexibility in representing the true geometry present in the field. Namely, the open ocean boundary can be extended into regions offshore where the forcing is known or will not significantly impact the nearshore circulation (e.g., Blain et al. 1994). The variable resolution afforded by this approach lends itself to the simulation of these larger domains without sacrificing mesh refinement in the nearshore region. Furthermore, the triangular mesh can easily capture to the geometric complexities of the coastal shoreline that often dictate nearshore circulation patterns.

Ongoing studies are focusing on including the influence of tide and wind forcing on nearshore wave-induced flows, and 3-D simulations that appropriately capture vertical mixing processes and the known vertical structure of the nearshore currents. An improved representation of wave-induced mixing is expected in the context of the 3-D model.

ACKNOWLEDGMENTS

REFERENCES

Allen, J.S., P.A. Newberger, and R.A. Holman, 1996. "Nonlinear Shear Instabilities of Alongshore Currents on Plane Beaches," *J. Fluid Mech.* **310**, 181-213.

Blain, C.A., J.J. Westerink, and R.A. Luettich, 1994. "The Influence of Domain Size on the Response Characteristics of a Hurricane Storm Surge Model," *J. Geophys. Res*. **99**(C9), 18467-18479.

Blain, C.A., J.J. Westerink, and R.A. Luettich, 1998. "Grid Convergence Studies on the Prediction of Hurricane Storm Surge," *Int. J. Num. Methods Fluids* **26**, 369-401.

Bowen, A.J. and R.A. Holman, 1989. "Shear Instabilities of the Mean Longshore Current," *J. Geophys. Res*. **94**(C12), 18,023-18030.

Church, J.C. and E.B. Thornton, 1993. "Effects of Breaking Wave Induced Turbulence Within a Longshore Current Model," *Coastal Eng*. **20**, 1-28.

Dodd, N., J. Oltman-Shay, and E.B. Thornton, 1992. "Shear Instabilities in the Longshore Current: A Comparison of Observations and Theory," *J. Phys. Oceanogr*. **22**, 62-82.

Ebersole, B.A. and R.A. Dalrymple, 1980. "Numerical Modeling of Nearshore Circulation," in *Proceedings of the Seventeenth Coastal Engineering Conference*, American Society of Civil Engineers, New York, NY, pp. 2710-2725.

Garcez Faria, A.F., E. Thornton, and T. Stanton, 1996. "A Quasi-3D Model of Longshore Currents," *Coastal Dynamics '95: Proceedings of the International Conference on Coastal Research in Terms of Large Scale Experiments*, W.R. Dally and R.B. Zeidler, eds., American Society of Civil Engineers, New York, NY, pp. 389-400.

Hagen, S.C., J.J. Westerink, and R.L. Kolar, 2000. "One-dimensional Finite Element Grids Based on a Localized Truncation Error Analysis," *Int. J. Num. Meth. Fl,* **32**, 241-261.

Hench, J.L. and R.A. Luettich, 1998. "Analysis and Application of Eulerian Finite Element Methods for the Transport Equation," in *Proceedings of the 5th International Conference on Estuarine and Coastal Modeling*, M. Spaulding and A. Blumberg, eds., American Society of Civil Engineers, Reston, VA, pp. 138-152.

Kinnmark, I.P.E., 1984. "The Shallow Water Wave Equations: Formulation, Analysis and Application," Ph.D. Dissertation, Department of Civil Engineering, Princeton University.

Kirby, J.T., 1986. "Higher-order Approximations in the Parabolic Equation Method for Water Waves," *J. Geophys. Res.* **91**, 933-952.

Kirby, J.T. and R.A. Dalrymple, 1994. *Combined Refraction/ Diffraction Model REF/DIF1, Version 2.5: Documentation and User's Manual, CACR Report No. 94-22*, Center for Applied Coastal Research, University of Delaware, Newark, DE, 171p.

Kolar, R.L. and W.G. Gray, 1990. "Shallow Water Modeling in Small Water Bodies," in *Proc. 8th Int. Conf. Comp. Meth. Water Res.* pp. 39-44.

Kolar, R.L., J.J. Westerink, M.E. Cantekin, and C.A. Blain, 1994a. "Aspects of Nonlinear Simulations Using Shallow Water Models Based on the Wave Continuity Equation," *Computers and Fluids* **23**, 523-538.

Kolar, R.L., W.G. Gray, J.J. Westerink, and R.A. Luettich, 1994b. "Shallow Water Modeling in Spherical Coordinates: Equation Formulation, Numerical Implementation, and Application," *J. Hydraul. Res.* **32**, 3-24.

Lippmann, T.C., T.H.C. Herbers, and E.B. Thornton, 1999. "Surf Zone Longshore Currents and Random Waves: Field Data and Models," *J. Phys. Oceanogr.* **29**, 231-239.

Longuet-Higgins, M.S. and R.W. Stewart, 1964. "Radiation Stresses in Water Waves: A Physical Discussion, with Applications," *Deep Sea Research* **11**, 529-562.

Longuet-Higgins, M.S., 1970a. "Longshore Currents Generated by Obliquely Incident Sea Waves, 1," *J. Geophys. Res.* **75**(33), 6778-6789.

Longuet-Higgins, M.S., 1970b. "Longshore Currents Generated By Obliquely Incident Sea Waves, 2," *J. Geophys. Res.* **75**(33), 6778-6789.

Luettich, R.A., J.J. Westerink, and N.W. Scheffner, 1992. *ADCIRC: An Advanced Three-Dimensional Circulation Model for Shelves, Coasts, and Estuaries, Report 1: Theory and Methodology of ADCIRC-2DDI* and *ADCIRC-3DL, Technical Report DRP-92-6*, U.S. Army Corps of Engineers Waterways Experimental Station, Vicksburg, MS.

Lynch, D.R. and W.G. Gray, 1979. "A Wave Equation Model For Finite Element Tidal Computations," *Comp. Fluids* **7**, 207-228.

McDougal, W.G. and R.T. Hudspeth, 1986. "Influence of Lateral Mixing on Longshore Currents," *Ocean Engng.* **13**(5), 419-433.

O'Connor, B.A. and D. Yoo, 1987. "Turbulence Modeling of Surf Zone Mixing," *Coastal Hydrodynamics*, R.A. Dalrymple, ed., American Society of Civil Engineers, New York, NY, pp. 371-386.

Özkan-Haller, H.T. and J.T. Kirby, 1999. "Nonlinear Evolution of Shear Instabilities," *J. Geophys. Res.* **104**(C11), 25,953-25,984.

Putrevu, U. and I.A. Svendsen, 1992. "Shear Instability of Longshore Currents: A Numerical Study," *J. Geophys. Res.* **97**(C5), 7283-7303.

Roach, P.J., 1994. "Perspective: A Method for Uniform Reporting of Grid Refinement Studies," *J. Fluid Eng.* **116**, 405-413.

Slinn, D.N., J.S. Allen, P.A. Newberger, and R.A. Holman, 1998. "Nonlinear Shear Instabilities of Alongshore Currents Over Barred Beaches," *J. Geophys. Res.* **103**(C9), 18,357-18,379.

Svendsen, I.A. and U. Putrevu, 1994. "Nearshore Mixing and Dispersion," in *Proc. R. Soc. Lond. A* **445**, 561-576.

Thornton, E.B. and R.T. Guza, 1986. "Surf Zone Longshore Currents and Random Waves: Field Data and Models," *J. Phys. Oceanogr.* **16**, 1165-1178.

Thornton, E.B. and C.S. Kim, 1993. "Longshore Current and Wave Height Modulation at Tidal Frequency Inside the Surf Zone," *J. Geophys. Res.* **98**(C9),16,509-16,519.

Van Dongeren, A.R. and I.A. Svendsen, 2000. "Nonlinear and 3D Effects in Leaky Infragravity Waves," *Coastal Engr.* **41**, 467-496.

Westerink, J.J., C.A. Blain, R.A. Luettich, and N.W. Scheffner, 1994a. *ADCIRC: An Advanced Three-Dimensional Circulation Model for Shelves, Coasts, and Estuaries, Report 2: User's Manual for ADCIRC-2DDI*, Technical Report DRP-92, Department of the Army.

Westerink, J.J., R.A. Luettich, and J.C. Muccino, 1994b. "Modeling Tides in the Western North Atlantic Using Unstructured Graded Grids," *Tellus* **46A**, 178-199.

Westerink, J.J., R.A. Luettich, J.K. Wu, and R.L. Kolar, 1994c. "The Influence of Normal Flow Boundary Conditions on Spurious Modes in Finite Element Solutions to the Shallow Water Equations," *Int. J. Num. Meth. Fl.* **18**, 1021-1060.

Whitford, D.J. and E.B. Thornton, 1996. "Bed Shear Stress Coefficients for Longshore Currents over a Barred Profile," *Coastal Eng.* **27**, 243-262.